Point Cloud Semantic Segmentation of Building Elements of Fatih Mosque, Istanbul

Khwlah KASEM AGHA **¹** , Can UZUN **²***

ORCID 1: 0009-0002-5880-299X
ORCID 2: 0000-0002-4373-9732
¹ Altınbas University, Graduate School of Science and Engineering, Department of Architecture, 34218, İstanbul, Türkiye.
² Altınbaş University, Faculty of Engineering and Architecture, Department of Architecture, 34218, İstanbul, Türkiye.
* e-mail*: can.uzun@altinbas.edu.tr*

Abstract

The architectural heritage digital model is important for high-accuracy documentation, archive security, and research opportunities. This study focuses on the autonomous documentation of the digital model of Fatih Mosque's facade elements. Fatih Mosque literature focuses on its restoration process, historical importance, and architectural values. The literature on the documentation of the mosque with current technological methods is limited. This study applies semantic segmentation on point-cloud data to detect facade elements. Point-cloud data was produced via photogrammetry from the southwest and northwest facades. The data was labeled with masonry wall, main load-bearing wall, column, window, entrance, staircase, arch, and spouts. CANUPO classifier in CloudCompare software is used for semantic segmentation. Changing the classification parameters in CANUPO increased the accuracy rate in predicting facade elements. This study contributes to the literature by providing autonomous documentation of the Fatih Mosque's facade and a guide for using the CANUPO classifier in digital model production.

Keywords: *Heritage digital models, point-cloud, semantic segmentation, photogrammetry, Fatih Mosque.*

İstanbul Fatih Camii'nin Nokta Bulutu Semantik Segmentasyonu

Öz

Mimari mirasın sayısal modellerinin üretilmesi, yüksek doğrulukta belgeleme, arşiv güvenliği, güncel yöntemlerle araştırma olanakları bakımından önemlidir. Bu çalışma Fatih Cami'nin cephe elemanlarının sayısal modellerinin otonom belgelenmesi sürecine odaklanmaktadır. Fatih Cami literatürü, caminin restorasyonu, tarihi önemi ve mimari değerleri konularını içermektedir. Caminin güncel teknolojik yöntemlerle belgelenmesi konusundaki literatür oldukça kısıtlıdır. Bu çalışmada Fatih Cami yapı elemanlarının otonom tespiti için nokta bulutu verisi ile anlamsal segmentasyon uygulanmıştır. Fatih Cami nokta bulutu verisi, caminin güneybatı ve kuzeybatı cephelerinden fotogrametri tekniği ile üretilmiştir. Nokta bulutu verisi, yığma duvar, ana taşıyıcı duvar, sütun, pencere, giriş kapısı, merdiven, kemer ve yağmur suyu oluğu yapı elemanları ile etiketlenmiştir. Anlamsal segmentasyon için CloudCompare yazılımındaki CANUPO sınıflandırıcı aracı kullanılmıştır. CANUPO ile sınıflandırma parametreleri düzenlenerek, farklı yapı elemanlarının tahminindeki doğruluk oranı arttırılabilmiştir. Bu çalışma hem Fatih Cami'nin cephe elemanlarının otonom belgelenmesi ile, hem de sayısal model üretiminde CANUPO sınıflandırıcı kullanımı için bir rehber niteliği oluşturarak literatüre katkı sağlamaktadır.

Anahtar kelimeler: *Sayısal miras modelleri, nokta bulutu, anlamsal bölütleme, fotogrametri, Fatih Cami.*

1. Introduction

Heritage building preservation is a universal topic essential for preserving cities' cultural identities and heritage assets. Heritage buildings also referred to as historical buildings, are irreplaceable structures that resemble events and stories of past generations (Penjor et al., 2024). Once lost, the portrayed identity and stories cannot be recovered (Solla et al., 2020). Therefore, regular assessments of heritage buildings are essential for their protection and conservation (Stober et al., 2018).

Assessing heritage structures requires surveyors' intervention to conduct research and site surveys by analyzing the building's condition through literature, historical records, and archives (Kuban, 2000). Hand-drawn survey drawings are produced upon conventional measuring tools such as tape measures, compasses, and leveling instruments (Karakus, 2020). With the advances of technology in heritage documentation, photographs started to be used for architectural documentation to manually gather visual data on the building's materials, size, and textures (Karakus, 2020; Korumaz & Dülgerler, 2011). Because using conventional methods for documentation is a tedious and time-consuming method, heritage building documentation is hard to manage manually (Baik, 2017). Recent methodologies utilizing digital three-dimensional (3D) representations of heritage buildings are essential to surpass the issues in conventional methods (Champion & Rahaman, 2019; Ergin, 2023). Digital heritage models represent existing historical buildings, which is a reliable data source that can be edited and shared (Grilli & Remondino, 2019; Maiwald et al., 2019). These models can be obtained in the form of meshes or point cloud models. Yang et al. (2023), defined point cloud models as 3D space models including massive geometric information consisting of points, where each point has its position, color, and reflection intensity. As shown in (Figure 1), digital heritage representations play a crucial role in heritage preservation, which can be used for documentation, representation, classification of building elements, and integration within the heritage building information modeling (HBIM) sector (Baik, 2017; Costantino et al., 2021; Clini et al., 2024; Martinelli et al., 2023; Nespeca et al., 2024; Shabani et al., 2022).
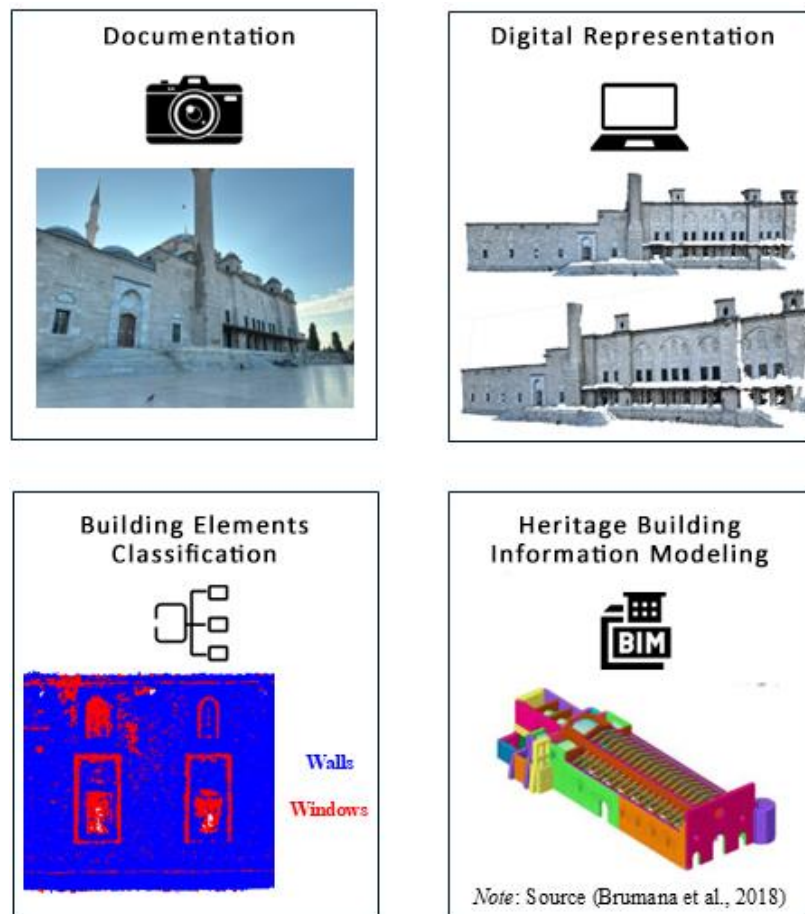

Figure 1. The importance and applications of digital heritage models within the heritage sector (by authors).

Moreover, it increases the efficiency of the decision-making process concerning renovation, maintenance, and evaluation (Croce et al., 2021; Macher et al., 2017; Pocobelli et al., 2018). Many literatures emphasize the importance and need of digital heritage models. Baik (2017) produced a digital model of a heritage house in Saudi Arabia, so it can be used in the database where information on heritage buildings and what should be restored or removed. Psomadaki et al. (2019), with the help of other professionals, focused on producing and documenting multiple heritage structures. Most studies on digital heritage are associated with BIM, referred to as Heritage BIM (HBIM). HBIM is a branch specialized in replicating heritage buildings and employing these models BIM software (Themistocleous et al., 2022).

More research is needed to represent heritage assets focusing on different architectural languages. For historical buildings in Turkey, multiple literature utilized the digitalization of historical buildings. Bianchini (2020) analyzed and surveyed the dome of Hagia Sophia by producing a digital point cloud model. Kan et al. (2019) used a laser scanner with a panoramic camera to capture the Suleymaniye mosque and utilized it in VR tours. For the main gate of Sehzade, Suleymaniye, and Atik Valide Mosques, Agirbas et al. (2022) captured the muqarnas ornaments for analysis and semantic segmentation. Regarding this literature, the Fatih mosque has received little attention on its preservation and digital documentation, even though it is one of Istanbul's important landmarks. Therefore, this study aims to produce a digital record of the Fatih Mosque, built between 1462 and 1470 and designed by the Architect Atik Sinan. By developing a point cloud model and semantically segmenting the Fatih mosque's façade elements.

1.1. Fatih Mosque Historical Significance

Fatih mosque as shown in (Figure 2), is a UNESCO World Heritage site located in the historical Fatih district in Istanbul/ Turkey which was part of a large complex that included schools, kitchens, and hospitals, built on a high hill. It was named after the conqueror Fatih Sultan Mehmet II, who conquered Istanbul in 1462 making it a remarkable historical monument within the city (Kunter & Ülgen, 1939, p. 5).

Figure 2. Fatih mosque in Istanbul / Turkey (by authors).

The historical significance of the Fatih Mosque lies in its original structure, which had distinct Ottoman architectural design principles, with the integration of elements suited to evolving styles (Eyice, 1995). Unfortunately, multiple devastating earthquakes occurred in Istanbul which resulted in the loss of the original mosque. In 1509, an earthquake named the "Little Apocalypse" destroyed big parts of the mosque's main domes and columns' capitals. Also, other parts were damaged in the 1557 and 1754 earthquakes. The biggest damage happened in 1765 when the mosque completely collapsed beyond alteration or repair (Kunter & Ülgen, 1939). This led to the rebuilding of the existing mosque which started in 1767 and ended in 1771.

Before, the mosque had an unsymmetrical plan design with a 26-meter-diameter dome and a semi-dome on one side, with two main spaces an open courtyard, and a prayer hall (Bal et al., 2015). According to Vatan (2018), the cause of the original mosque's collapse is the unsymmetric plan design. Now, the current mosque has a symmetrical plan design and exterior layout, with a 19 m dome

surrounded by semi-domes on four sides resting on four arches, supported by four pillars which provide an equal load distribution system.

The essence of the classical Ottoman style remained in the mosque's current style, particularly shown in its domes and two minarets, each with three balconies, built from stone and marble. The exterior façade element features several wooden entrances, three leading into the open courtyard and another three leading to the prayer hall. The design also incorporates a main dome elevated on a higher level, rectangular lower windows, pointed arched upper windows, and open courtyards surrounded by corridors shaded by small domes. These elements are found in many other mosques across Istanbul, highlighting the need to have digital records of the mosque's building elements for analysis and observations.

Originally, the mosque represented early Ottoman architecture also in its minarets and domes design. But it had rectangular and pointed arch windows, along with columns and doorways all arranged in a regular layout and harmony. However, the current mosque adopts a simpler and more static style influenced by Baroque architecture (Kunter & Ülgen, 1939, p. 9). According to limited literature, the mosque was built on the remaining foundations of the ancient Havarion Church from the Byzantine era (Ceylan & Ocakcan, 2013; Eyice, 1995). Despite this, the Fatih Mosque had distinct Ottoman architectural design elements where no trace of Byzantine art was evident, unlike other mosques in Istanbul (Eyice, 1995).

The main northwestern façade of the current mosque, measured from Google Earth, spans 60 meters. It features six lower rectangular windows, six upper pointed arch windows, and a marble entrance that leads directly to the courtyard which remained because it wasn't affected by earthquakes (Kunter & Ülgen, 1939, p. 1). The longer facades, the southwest and northeast, each measure 95 meters and feature a total of 28 rectangular windows, 17 pointed arch windows, and two wooden entrances that lead to the courtyard and prayer hall. On the other hand, the northeastern side has 19 rectangular windows and 24 pointed arch windows, but no entrances. This side is inaccessible due to its proximity to a graveyard that has the tombs of Sultan Mehmed II and his consort, Gülbahar Hatun. Additionally, it faces the domed Carullah Efendi Library.

Given the historical significance of the mosque, there is limited literature addressing the reasons behind its multiple collapses and the methods used for its preservation. (Table 1) highlights key aspects from previous studies on the conservation efforts for the Fatih Mosque.

Table 1. Comparison between the literature conducted on the preservation of the Fatih mosque (by authors)

Referenced Literature	Year	Focus	Methodology	Findings
(Vatan, 2018)	2018	Examined the structural system of the domes.	-Studied construction techniques. -Analyzed past damages records.	Structural issues were reported regarding to the asymmetrical design of the original plan and the thin exterior walls.
(Akyuz et al., 2015)	2015	Analyzed the type of plaster and mortar used in the wall painting.	Used EDXRF micro-Raman and FTIR analyzing techniques.	Concluded that the plaster mortars belong to the mixed lime–gypsum mortar group.
(Beyen, 2008)	2008	Identified structural problems after the earthquake.	Utilized a digital converter, DT-2827 A/D board with 16-bit A/D converter at a high speed of 100 kHz accommodating.	Graphs and records were produced on the mosque's past, present, and future structural behavior.
(Berilgen, 2007)	2007	Studied the local soil condition. Predicted the site's future behavior for future earthquakes.	Employed horizontal/vertical FAS ratios and bedrock input motion to test future behaviors.	Concluded that the soil had a significant impact on the structural damage experienced during previous earthquakes.

Table 1. (Continued) Comparison between the literature conducted on the preservation of the Fatih mosque (by authors)

(Yastıklı & Alkıs, 2003)	2003	Documented the existing mosque using close-range photogrammetry.	Took 230 photographs with a semi-metric Rolleiflex 6008 tool.	A 3D model of the Fatih Mosque was created, using vector and raster data.
(Kunter & Ülgen, 1939)	1939	Studied the history of the mosque and gathered valuable information.	-Analyzed visual and written records including drawings and manuscripts.	Found valuable information on the old mosque structure before it collapsed.

Despite the literature highlighting the Fatih Mosque's exposure to severe damage over the years, there remains a significant gap in the utilization of advanced technologies and research focused on its digital documentation and preservation. This gap is due to the loss of the mosque's original structure, which was not properly documented during the rebuilding phase. Therefore, this research aims to address two objectives: first, creating a point cloud model for two of the Fatih mosque's facades, and second, semantically segmenting these models to extract facade elements.

By achieving these objectives, the study will contribute to:

1. Establishing the first step of a long-term heritage conservation strategy, using digital documentation.
2. Generating data trained on the Fatih Mosque that can be used for the segmentation of similar architectural elements in other mosques with an Ottoman architectural style.
3. Providing a shareable digital model that can be utilized by various professionals.
4. Streamlining the workflow for data acquisition and building element detection through digitalization.

To tackle the digitalization of the mosque, employing point cloud semantic segmentation for the mosque's elements offers an innovative solution for a large structure.

1.2 Role of Point Cloud Semantic Segmentation in Heritage Analysis

Point cloud semantic segmentation (PCSS) is a widely researched topic that simplifies heritage digital documentation. PCSS is a supervised learning process in which the trained algorithm decides the semantic labels of each point in the point cloud with the training labels. Machine learning (ML) and deep learning (DL) methods can be used in PCSS problems. While ML classifies observations using manually selected features, DL automatically extracts and classifies features. For PCSS, several DL algorithms can be listed, such as PointNet (Qi et al., 2017), PointNet++ (Qi et al., 2017), and DGCNN (Pierdicca et al., 2020). On the other hand, in addition to the supervised methods, ML algorithms include unsupervised methods (without labels training) such as region-growing (Nurunnabi, Belton & West, 2012), clustering-based segmentation (Galantucci & Fatiguso, 2019), and edge-based classifier (Rabbani et al., 2006).

Semantic segmentation for heritage buildings refers to interpreting digital heritage data by segmenting building elements as separate objects that can be developed, analyzed, and imported into modeling software (Rocha et al., 2020). It involves classifying unstructured points into meaningful groups and assigning a label to describe each group (Xie et al., 2020). These labels represent different building elements, such as walls, columns, and doors. In this study's case, semantic labels are the facade elements of the Fatih Mosque.

PCSS offers advantages, including detailed interpretation of raw point cloud models by classifying elements within the captured scene (Macher et al., 2017). Moyano et al. (2021) applied PCSS to extract structural elements and conduct a structural analysis of La Anunciación church. Also, PCSS Groups unstructured data into labeled clusters, enabling the development of parametric objects that can be imported into BIM programs (Moyano et al., 2021). Barrile and Fotia (2022) experimented with the PCSS of a church in Italy captured using UAVs and laser scanners to extract different elements into editable parametric objects. Moreover, PCSS and digital models minimize the risk of data loss or

misrepresentation caused by human interventions by ensuring that heritage treasures are preserved and passed on to future generations.

Some classification algorithms are deployed as tools for ease of classification algorithm use. CANUPO is one such tool, a plugin within the CloudCompare software. CANUPO will be further elaborated in this research using the Fatih Mosque as a case for PCSS. In CANUPO, one can quickly train classification algorithms without hypertuning the training parameters to get accurate results. Therefore, the CANUPO tool was selected for the PCSS task of this study for ease of use.

The following chapter explains the methodology employed for the semantic segmentation of the Fatih Mosque's building elements.

2. Material and Method

This section describes the workflow used for the semantic segmentation of the point cloud model of the Fatih mosque. Despite the steps illustrated in (Figure 3), It is important to note that this workflow is not strictly linear, some steps may be repeated, skipped, or tested several times.
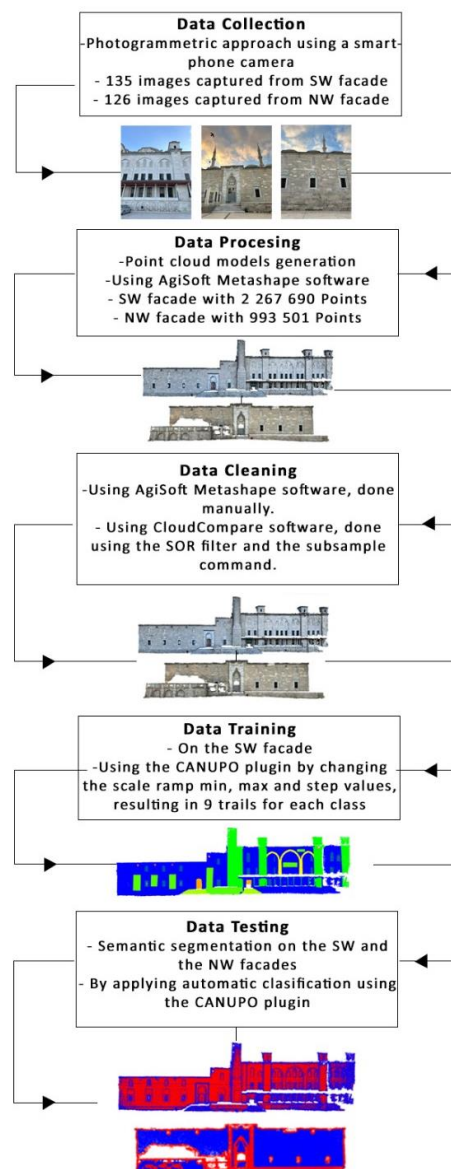
Data Collection
-Photogrammetric approach using a smart-phone camera
- 135 images captured from SW facade
- 126 images captured from NW facade

Data Procesing
-Point cloud models generation
-Using AgiSoft Metashape software
- SW facade with 2 267 690 Points
- NW facade with 993 501 Points

Data Cleaning
-Using AgiSoft Metashape software, done manually.
- Using CloudCompare software, done using the SOR filter and the subsample command.

Data Training
- On the SW facade
-Using the CANUPO plugin by changing the scale ramp min, max and step values, resulting in 9 trails for each class

Data Testing
- Semantic segmentation on the SW and the NW facades
- By applying automatic clasification using the CANUPO plugin

Figure 3. Workflow for the semantic segmentation of the Fatih mosque's point cloud model (by authors).

The first step is data collection, which requires site visits and equipment to capture the existing structure. For this study, photogrammetry was employed by using a smartphone camera to capture the Southwestern (SW) and Northwestern (NW) facades. In the second step, the captured images were

processed using Agisoft Metashape Pro software to generate a 3D point cloud model. After data processing, data cleaning was applied using manual techniques and commands within CloudCompare. Fourth, is data training on the SW side through manual identification of areas representing the mosque's elements. Last comes the classifier testing, by assessing the CANUPO plugin's ability to segment the elements from the NW facade, based on the trained data on the SW facade.

2.1. Dataset

The dataset consists of two-point cloud models. The SW façade model is used for training, and the NW façade is used for testing, as illustrated in (Figure 4). The study was limited to the SW and the NW facades because the remaining sides couldn't be accessed and captured. The Northeastern facade has a tomb in front of it, and the southeastern facade was covered for renovation.
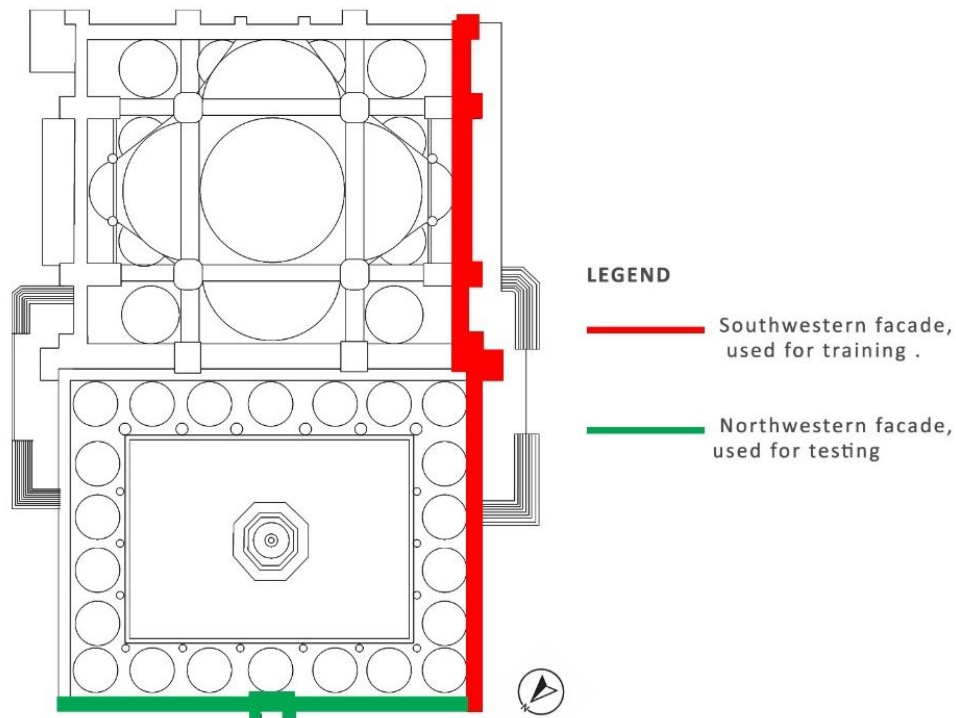
Figure 4. Indication of the facades used for training and testing for semantic segmentation (by authors).

The segmentation classifier was trained on the SW facade which has more of the targeted elements for segmentation. The training procedure helped the classifier learn the Faith Mosque's features. After training, the NW facade was used for testing the plugin's performance. This process helps conduct a deeper analysis of each element while understanding the overall structure.

2.2. Data Collection and Point Cloud Processing for Fatih Mosque

To prepare the dataset for semantic segmentation, data collection, processing, and cleaning were performed.

2.2.1. Data collection

Data collection was conducted using a photogrammetric approach of an iPhone 14 ProMax smartphone camera. This limited the study to be conducted at eye-level height excluding higher elements like the minarets and domes. The site was visited several times ensuring that the area wasn't crowded, and the sun wasn't harsh. All visits were at 7 a.m. when the sun wasn't strong creating harsh shadows. Another consideration was image alignments, to ensure better point cloud generation, sequential images were captured following a horizontal pace taken at different distances. (Table 2) displays sample images captured at different distances from both facades.

Table 2. Sample images captured at different distances from the Fatih mosque's Southwest and Northwest facades (by authors)

	Images captured at 8 meters	Images captured at 15 meters	Images captured at 20 meters
Images captured from the Southwestern Facade			
	Images Captured at 3 meters	**Images Captured at 8 meters**	**Images Captured at 13 meters**
Images captured from the Northwestern Facade			

The farthest distance was captured 13 to 20 meters away, the closest distance was 3 to 8 meters away to capture clearer details and textures. In total, 261 images were taken, 135 images from the SW facade and 126 images from the NW facade.

2.2.2. Data processing

For point cloud generation, Agisoft Metashape Pro software was used. Agisoft Metashape, is a photogrammetry processing software (Agisoft, 2019). It aligns photos taken from different angles, then finds sharable points (tie points) and aligns them to create a continuous scene. Then, it creates a sparse point cloud model which can be converted into a dense model. To perform semantic segmentation, it is necessary to build a dense point cloud model because it portrays in-depth information and textures.

In this study, 135 images of the SW facade were imported within Agisoft Metashape. After importing, the align photos command was applied. This command automatically detected common points and aligned them according to shared features. 135/ 135 images were successfully aligned. After alignment, the build dense cloud feature was employed to generate a rich model displaying all the elements, as shown in (Figure 5).

Figure 5. A 2 267 690 point cloud model of the SW facade, captured from Agisoft Metashape (by authors).

The model was exported in medium resolution, to have a manageable dataset because this study focuses on capturing the main building elements rather than ornaments and smaller details. The consideration reduced the training and segmentation time significantly. The same process was employed for generating the NW model, as portrayed in (Figure 6).

Figure 6. A 993 501 point cloud model of the NW facade, captured from Agisoft Metashape (by authors).

A partial part of the NW facade failed to be represented because it comes behind balustrades which affected the generated model. To have manageable models, data-cleaning techniques were applied.

2.2.3. Data cleaning

Data cleaning using Agisoft Metashape software in addition to techniques within the CloudCompare software was applied. CloudCompare is open-source software used for processing and classifying point cloud models which doesn't require professionals to operate it, and it is compatible with data collected from both laser scanners and photogrammetry.

First, the SW model was manually cleaned in Agisoft Metashape using the rectangular selection tool, to delete unnecessary points like points of the sky. The cleaned model was exported in .las format into the CloudCompare software. In CloudCompare, the Statistical Outlier Removal (SOR) filters out noise points by calculating the average distance between each point and its neighbors, where points far from the average distance are deleted. Before the SOR, the model had 2 615 530 points, then it had 2 520 140 points. The third technique is subsampling. This feature randomly samples by minimizing the number of points based on a specified ratio. A small ratio of 0.01 m was set, to maintain an accurate representation without losing details. After subsampling the points were reduced to 2 267 690 points. For the NW facade, only manual cleaning was applied. Despite the efficiency of the techniques within CloudCompare, the point cloud model of the NW facade had a small number of points below a million. When the SOR and the subsampling feature were applied, the points were reduced from 993 501 to 570 498 points, which removed almost half of the points. Therefore, the model had 998 872 points and was reduced to 993 501 points by manual cleaning. To conclude, a total of 347 840 points from the SW facade were removed, and 5 371 points from the NW facade. These steps play an important role in controlling large datasets and ensuring smoother classification of the Fatih mosque's façade elements.

2.2.4 Ontological Typology of the Fatih Mosque Façade Elements

An ontology was created to describe the Fatih mosque's facade elements. This ontology was developed according to Fatih mosque's structural elements, based on the ontology created by (Stouffs & Tunçer, 2015), where they described physical and conceptual elements of mosques within the Ottoman era. (Figure 7) decomposes the exterior façade elements, in which every element has an additional level of detail that belongs to it.
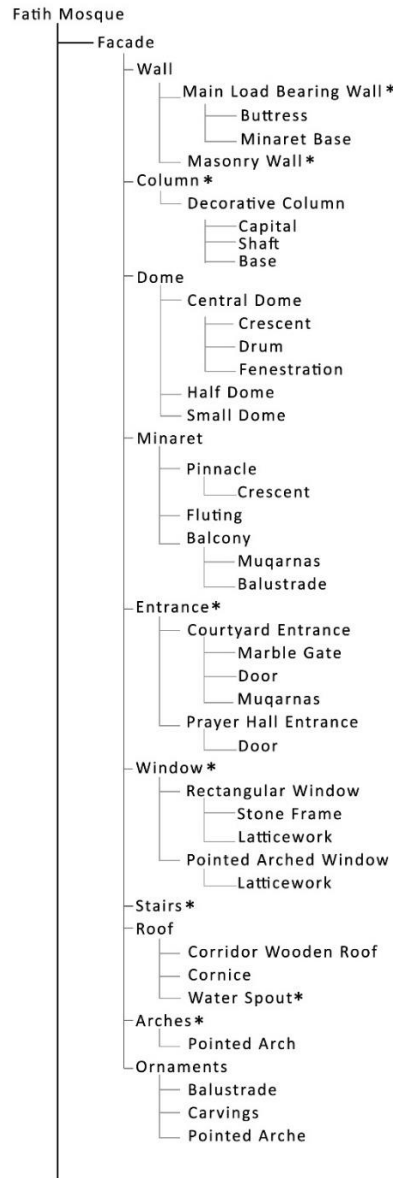
```
Fatih Mosque
├── Facade
    ├── Wall
    │   ├── Main Load Bearing Wall *
    │   │   ├── Buttress
    │   │   └── Minaret Base
    │   └── Masonry Wall *
    ├── Column *
    │   └── Decorative Column
    │       ├── Capital
    │       ├── Shaft
    │       └── Base
    ├── Dome
    │   ├── Central Dome
    │   │   ├── Crescent
    │   │   ├── Drum
    │   │   └── Fenestration
    │   ├── Half Dome
    │   └── Small Dome
    ├── Minaret
    │   ├── Pinnacle
    │   │   └── Crescent
    │   ├── Fluting
    │   └── Balcony
    │       ├── Muqarnas
    │       └── Balustrade
    ├── Entrance *
    │   ├── Courtyard Entrance
    │   │   ├── Marble Gate
    │   │   ├── Door
    │   │   └── Muqarnas
    │   └── Prayer Hall Entrance
    │       └── Door
    ├── Window *
    │   ├── Rectangular Window
    │   │   ├── Stone Frame
    │   │   └── Latticework
    │   └── Pointed Arched Window
    │       └── Latticework
    ├── Stairs *
    ├── Roof
    │   ├── Corridor Wooden Roof
    │   ├── Cornice
    │   └── Water Spout *
    ├── Arches *
    │   └── Pointed Arch
    └── Ornaments
        ├── Balustrade
        ├── Carvings
        └── Pointed Arche
```

Figure 7. An ontology for the Fatih mosque's façade elements. Elements marked with an asterisk (*) are used for training and semantic segmentation (by authors).

Eight distinct categories were identified, since the objective of this study is to digitalize the Fatih mosque and extract its elements, the categories were chosen with a focus on the main elements instead of ornaments and details. Categories like masonry walls, main load bearing walls, columns, entrances, windows, stairs, arches, and waterspouts were identified. Elements like domes and minarets weren't chosen because they weren't a part of the captured scene. Another important aspect to clarify is the minaret base element categorization, since only the base was captured, it was categorized as a sub-element within the main load bearing walls because it is a foundational element that shares the same characteristics of the buttresses that are attached to masonry load bearing walls. Based on the eight elements, semantic segmentation using the CANUPO plugin in CloudCompare was utilized.

2.3. Semantic Segmentation Using CANUPO Plugin

CANUPO plugin was employed for semantic segmentation of the SW and NW facades. CANUPO is a plugin in CloudCompare used for classifying point cloud models (Brodu & Lague, 2012). It classifies based on a multi-scale dimensionality criterion, which distributes multiple core points, and recognizes patterns surrounding each point according to a scale ramp value of a minimum (min), maximum (max), and step value. The min value is the smallest range the plugin analyzes around a point, the max is the biggest range, and the step refers to the increments between the min and max ranges. However, the plugin only performs binary classification by classifying points into two groups (façade - windows). The classification process contains two phases: training the classifier and classifying. In the training phase, the process starts with the manual identification of sample areas representing each element. Then, the main cloud model is separated into multiple clouds (classes). Then, the "train classifier" command is applied, in this step, two classes are chosen (class 1 and class 2) representing (facade and windows) as an example. According to the targeted element, the scale ramp values are set. The classifier then results in a classifier file in .prm format. This file is used for classification.

In this study, the training phase was performed on the SW facade. It started with the manual identification of sample areas. Using the segment tool, a polyline was manually drawn around each element's representative area as shown in (Figure 8).
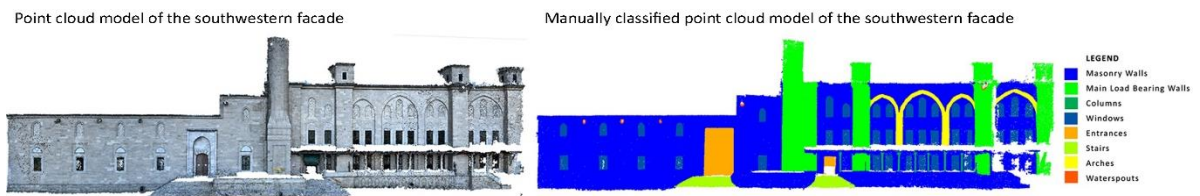
Figure 8. Manually selected sample areas representing the Fatih mosque's façade elements (by authors).

To export the selected areas as separate classes, the "split cloud according to the integer values" from the scalar field command was applied. This resulted in multiple clouds, where each cloud represents an element. After manual identification, the "train classifier" feature was used. For each targeted element, 9 experiments with the scale ramp values (min, max, and step) were conducted. Each time, two constant values were kept constant while changing the third value. After every trial, a classifier file was produced with a total of 9 classifier files for each class, then every classifier was used to classify the mosque's elements from the SW facade, as shown in (Table 3).

Table 3. CANUPO's training trails on the SW facade, based on changing the scale ramp min, max, and step values. Only scale values marked with an asterisk (*****) symbol were used for testing (by authors).

Class	Value	Segmentation Results		
Windows	Max	Min: 0.2, Step: 0.4, Max: 0.6	Min: 0.2, Step: 0.4, Max:0.8 *	Min: 0.2, Step: 0.4, Max: 1.0
	Step	Min: 0.2, Step: 0.3, Max: 0.8	Min: 0.2, Step: 0.4, Max: 0.8	Min: 0.2, Step: 0.6, Max: 0.8
	Min	Min:0.08, Step: 0.4, Max: 0.8	Min: 0.2, Step: 0.4, Max: 0.8	Min: 0.3, Step:0., Max: 0.8

Table 3. (Continued) CANUPO's training trails on the SW facade, based on changing the scale ramp min, max, and step values. Only scale values marked with an asterisk (*****) symbol were used for testing (by authors)*.*
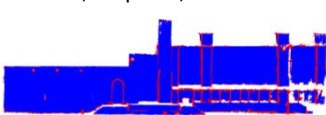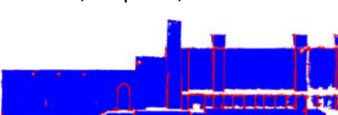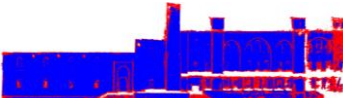
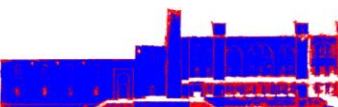|		Min:0.2, Step: 0.4, Max: 0.6	Min: 0.2, Step: 0.4, Max: 0.8	Min: 0.2, Step: 0.4, Max: 1.0
Masonry Walls	**Max**			
		Min: 0.2, Step: 0.3, Max: 0.8	Min: 0.2, Step: 0.4, Max: 0.8	Min: 0.2, Step: 0.6, Max:0.8
	Step			
		Min: 0.08, Step:0.6, Max: 0.8	Min: 0.2, Step: 0.6, Max: 0.8 *****	Min: 0.4, Step: 0.6, Max: 0.8
	Min			
Columns		Min: 0.2, Step: 0.6, Max: 1.0	Min: 0.2, Step: 0.6, Max: 0.8	Min: 0.2, Step: 0.6, Max: 1.2 *****
	Max			
		Min: 0.2, Step: 0.6, Max: 1.2	Min: 0.2, Step: 0.8, 1.2	Min: 0.2, Step: 1.0, Max: 1.2
	Step			
		Min: 0.2, Step: 0.8, Max: 1.2	Min: 0.4, Step: 0.8, Max: 1.2	Min: 0.6, Step: 0.8, Max: 1.2
	Min			
Stairs		Min: 0.2, Step: 0.4, Max: 0.6	Min: 0.2, Step: 0.4, Max: 0.8 *****	Min: 0.2, Step: 0.4, Max: 1.2
	Max			
		Min: 0.2, Step: 0.4, Max: 0.8	Min: 0.2, Step: 0.3, Max: 0.8	Min: 0.2, Step: 0.6, Max: 0.8
	Step			
		Min: 0.2, Step: 0.4, Max: 0.8	Min: 0.08, Step: 0.4, Max: 0.8	Min: 0.06, Step: 0.4, Max: 0.8
	Min			

Table 3. (Continued) CANUPO's training trails on the SW facade, based on changing the scale ramp min, max, and step values. Only scale values marked with an asterisk (*****) symbol were used for testing (by authors)*.*
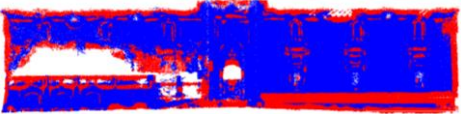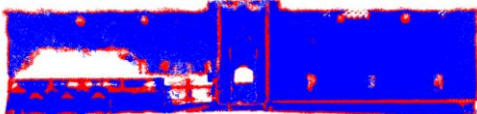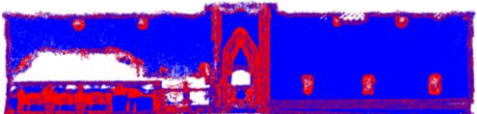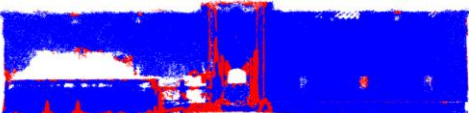
		Min: 1.0, Step: 1.2, Max: 2	Min: 1.0, Step: 1.2, Max: 1.6	Min: 1.0, Step: 1.2, Max: 2.6
Main Load Bearing Walls	**Max**			
		Min: 1.0, Step: 1.4, Max: 2.0	Min: 1.0, Step: 1.6, Max: 2.0	Min: 1.0, Step: 2.0, Max: 3.5
	Step			
		Min: 0.6, Step: 1.2, Max: 2	Min: 0.8, Step: 1.2, Max: 2	Min: 1.1, Step: 1.2, Max: 2 *****
	Min			
Arches		Min: 0.2, Step: 0.4, Max: 0.6	Min: 0.2, Step: 0.4, Max: 0.8	Min: 0.2, Step: 0.4, Max: 1.0
	max			
		Min: 0.2, Step: 0.3, Max: 0.8	Min: 0.2, Step: 0.4, Max: 0.8	Min: 0.2, Step: 0.6, Max: 0.8
	step			
		Min: 0.08, Step: 0.4, Max: 0.8	Min: 0.2, Step: 0.3, Max: 0.8	Min: 0.3, Step: 0.4, Max: 0.8 *****
	min			
Entrances		Min: 0.4, Step: 0.6, Max: 0.8	Min: 0.4, Step: 0.6, Max: 1.2	Min: 0.4, Step: 0.6, Max: 0.7
	Max			
		Min: 0.4, Step: 0.5, Max: 0.8	Min: 0.4, Step: 0.6, Max: 0.8	Min: 0.4, Step: 0.7, Max: 0.8 *****
	Step			
		Min: 0.2, Step: 0.7, Max: 0.8	Min: 0.4, Step: 0.7, Max: 0.8	Min: 0.6, Step: 0.7, Max: 0.8
	Min			

Table 3. (Continued) CANUPO's training trails on the SW facade, based on changing the scale ramp min, max, and step values. Only scale values marked with an asterisk (*****) symbol were used for testing (by authors)*.*

The numbers in the table, such as 0.2 or 1.2, represent distances in meters that the plugin analyzes. These trials were essential for identifying the best classification parameters for each element while observing the influence of the scale ramp on the classification results. Among the nine trials conducted for each class, the scale ramp parameter that resulted in the best classification results on the trained data was exported into a classifier file. This classifier was then used to test the plugin's performance on the elements of the NW facade, providing insight into its ability to detect the same elements in unseen data. The segmentation results applied to the NW facade are presented in (Table 4).

Table 4. Segmentation results on the testing dataset on the NW façade (by authors).

Class	Segmentation Results
Windows	
Masonry Walls	
Stairs	
Entrance	
Arches	
Waterspouts	

This workflow was repeated several times to achieve the best results by adjusting the scale ramp to the suitable values. The presented semantic segmentation outcomes formed the basis of the following assessment chapter.

2.4 Assessment of the CANUPO's Classifier Performance

CANUPO's plugin's results were evaluated based on the classification evaluation metrics, which are accuracy, recall, precision, and false positive rate (FPR). This method aims to provide a reliable measure of the plugin functionality in detecting the Fatih mosque's facade elements. Applying this assessment gives an understanding of the classifier's performance.

2.4.1   Identification of ground truth points

To identify the ground truth points (GTP), the manually selected representative areas illustrated before (Figure 8), represent GTP. These points resemble the number for each element, in which cautious manual selection was done to ensure optimal representation of the element. After the identification of GTP for each class, the resulting numbers were recorded.

2.4.2   Calculation of TP, FP, FN, TN points

In machine learning, each classification results in 4 types of points under the name of a confusion matrix, this matrix includes True Positive (TP), True Negative (TN), False Positive (FP), and False Negative (FN) points. (TP) are positive points that belong to the segmented class, and they were correctly classified. (FP) are positive points that are actually negative but were incorrectly classified. (FN) are negative points that are actually positive but were incorrectly classified. (TN) are negative points that don't belong to the segmented class, and they were correctly classified.

After the identification of GTP, the TP points were identified. Because CANUPO only performs binary segmentation, each segmentation consists of two classes, the targeted element and the facade. By using the split cloud according to the integer values command, each class can be analyzed separately. Accordingly, the targeted element's result is a combination of TP and FP points. To extract the TP points, manual selection of the same representative areas of the GTP was identified. To extract the FP points, equation (1) was used.

$$FP \ = \ Total \ Number \ of \ Points \ from \ the \ Targeted \ Element - TP \ (1)$$

The other class in the binary classification, the facade, is a combination of FN and TN points. To calculate the FN points, equation (2) was used, this was employed because the manually selected areas of the GTP are a combination of TP and FN.

$$FN \ = \ GTP - TP \ (2)$$

Lastly, to calculate the TN, the FN points were subtracted from the façade's points, as shown in equation (3).

$$TN \ = \ Total \ Number \ of \ the \ Facade's \ Points - FN \ (3)$$

Using these formulas in combination with manual identification, the GTP, TP, FP, TN, and FN points were calculated. (Table 5) displays the confusion matrix point numbers according to each segmented facade element.

Table 5. Number of GTP, and points within the confusion matrix including TP, FP, TN, and FN points based on each element's segmentation result (by authors).

	Segmented Class	GTP	TP Points	FP Points	TN Points	FN Points
	Masonry Walls	1 280 605	726 995	537 633	553 610	449 452
Southwestern Facade	Main Load Bearing Walls	548 764	211 239	216 848	337 525	1 502 078
	Columns	19 817	19 228	235 219	589	2 012 654
	Windows	200 196	167 042	605 421	33 154	1 462 073
	Entrances	75 617	50 691	652 435	24 926	1 539 638

Table 5. (Continued) Number of GTP, and points within the confusion matrix including TP, FP, TN, and FN points based on each element's segmentation result (by authors).

	Stairs	88 106	77 501	443 172	10 605	1 736 412
	Arches	47 442	35 346	581 765	12 096	1 638 483
	Waterspouts	7 143	7 023	198 526	120	2 062 021
Northwestern Facade	Masonry Walls	811 469	626 873	99 905	184 596	82 127
	Windows	41 698	22 888	290 299	18 810	661 504
	Entrances	118 610	91 736	304 246	26 874	570 645
	Stairs	14 749	5 462	183 565	9 287	795 587
	Arches	5 409	5 328	276 629	81	711 463
	Waterspouts	1 575	0	115701	1 575	876 225

2.4.3. Accuracy, recall, precision, and false positive rate percentage calculation

To calculate the evaluation metrics for each class, equations (4), (5), (6), and (7) are referenced from Macher, Landes, and Grussenmeyer (2017). For accuracy, equation (4) is used to measure the overall performance of the classifier, assessing its ability to correctly identify positive and negative points.

$$Accuracy = \frac{TP+TN}{TP+TN+FP+FN} \times 100\% \text{ (4)}$$

The recall (True Positives Rate) is calculated to evaluate the number of positive points correctly classified. Using equation (5) the recall was obtained.

$$Recall = \frac{TP}{TP+FN} \times 100\% \text{ (5)}$$

The precision metric evaluates how many of the predicted positive points were actually positive, testing the accuracy of the classifier's predictions, using equation (6).

$$Precision = \frac{TP}{TP+FP} \times 100\% \text{ (6)}$$

Lastly, the False Positive Rate (FPR), determined using equation (7), measures the proportion of actual negatives that were misclassified as positives.

$$False\ Positive\ Rate = \frac{FP}{FP+TN} \times 100\% \text{ (7)}$$

To interpret the percentages, a range of high, medium, and low ranges were set: values above 75% were classified as high, 50–75% as medium, and below 50% as low. However, some limitations need to be considered. First, the identification of Ground Truth Points (GTP) and True Positive (TP) points is done manually, which was subjected to errors due to the complexity of managing the dataset manually. However, to avoid so many errors, the representative areas were selected as accurately as possible. Second, since the NW facade wasn't used for training, its representative areas had to be identified manually too, to calculate the evaluation metrics using the same mentioned equations. Third, for the masonry walls class, the number of GTP and TP points include additional ornamental elements like the stone carvings above the windows, which aren't targeted for classification. Nonetheless, this didn't impact on the evaluation process.

3. Findings and Discussion

This chapter presents the findings from the CANUPO classifier. The classifier was trained to extract eight building elements. (Table 6) displays the assessment evaluation percentages of the CANUPO's classifier segmentation results.

Table 6. Accuracy, recall, precision, and false positive rate percentages for the segmented classes (by authors).

	Targeted Class	Accuracy Percentage	Recall Percentage	Precision Percentage	False Positive Rate Percentage
Southwestern Facade	Masonry Walls	52%	57%	57%	54%
	Main Load Bearing Walls	76%	38%	49%	13%
	Columns	90%	97%	8%	10%
	Windows	72%	83%	22%	29%
	Entrances	70%	67%	7%	30%
	Stairs	80%	88%	15%	20%
	Arches	74%	75%	6%	26%
	Waterspouts	91%	98%	3%	9%
Northwestern Facade	Masonry Walls	71%	77%	86%	55%
	Windows	69%	55%	7%	30%
	Entrances	67%	77%	23%	35%
	Stairs	81%	37%	3%	19%
	Arches	72%	99%	2%	28%
	Waterspouts	88%	0%	0%	12%

The accuracy metric indicates the classifier's general ability to detect the TP and TN points. Therefore, based on the chosen scale ramp values from (Table 4) and the accuracy metric, the results were assigned with a high, medium, and low range in (Table 7). The targeted element is classified in red, while the façade is always classified in dark blue.

Table 7. Categorization of the classification results in high, medium, and low accuracy, based on the accuracy metric percentages (by authors).
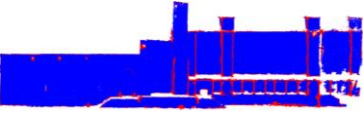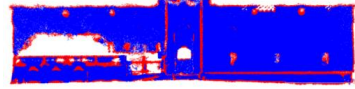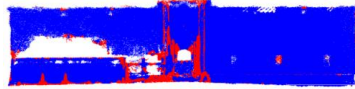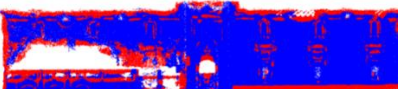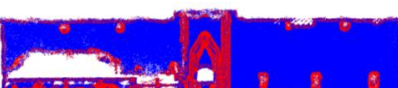
Accuracy Metric-Based Categorization		
High Accuracy (above 75%)	Medium Accuracy (50 – 75%)	Low Accuracy (Below 50%)
Southwestern Façade		
Main Load bearing walls Class	Masonry Walls Class	-
Columns Class	Windows Class	-
Stairs Class	Entrances Class	-

Table 7. (Continued) Categorization of the classification results in high, medium, and low accuracy, based on the accuracy metric percentages (by authors).

Waterspouts Class	Arches Class	-

Northwestern Façade

Stairs Class	Masonry Walls Class	-

Waterspouts Class	Windows Class	-

-	Entrances Class	-

-	Arches Class	-

Larger elements with a broader scale ramp like the main load-bearing walls, with a 1.1 min, 1.2 step, 2 max, and the columns from the SW facade, have a higher accuracy. On the other hand, the scale ramp with narrower values below 1 meter, had high and medium accuracy, yet no element resulted in a low accuracy from both facades. Accuracy gives a general insight without explanation of what was correctly classified and misclassified. Therefore, analyzing other metrics is essential.

3.1 Southwestern Facade Evaluation Metrics

- Masonry Walls Class
    - *Accuracy: 52% (Medium), Recall: 57% (Medium), Precision: 57% (Medium), FPR: 54% (Medium)*

This class illustrates moderate performance in identifying the TP and TN points. Even though the masonry walls can be easily distinguished from the segmentation result, the medium recall and precision demonstrate failure in detecting half of the correct points. Also, 54% of the FPR suggests that almost half of the points were incorrectly classified.

- Main Load Bearing Walls Class
    - *Accuracy: 76% (High), Recall: 38% (Low), Precision: 49% (Low), FPR: 13% (Low)*

While the accuracy is close to high, the very low recall and precision indicate that many TP points were missed, and half of the predicted points were wrong. The increased accuracy relates to the low FPR, where the classifier made fewer mistakes in classifying non-targeted elements.

- Columns Class
    - *Accuracy: 90% (High), Recall: 97% (High), Precision: 8% (Low), FPR: 10% (Low)*

The high accuracy and recall suggest that almost all columns were correctly segmented. However, the low precision indicates that a high number of points were mistaken with them.

- Windows Class
  - *Accuracy: 72% (Medium), Recall: 83% (High), Precision: 22% (Low), FPR: 29% (Low)*

Accuracy indicates moderate performance, with a high recall meaning that a high number of TP points were classified. However, the 22% precision says that many points were confused with the windows' points.

- Entrances Class
  - *Accuracy: 70% (Medium), Recall: 67% (Medium), Precision: 7% (Low), FPR: 30% (Low)*

The medium accuracy and recall prove moderate performance. The low FPR shows that CANUPO had fewer false tempts in classifying non-targeted elements, this might be because of the entrance's distinct geometry and material.

- Stairs Class
  - *Accuracy: 80% (High), Recall: 88% (High), Precision: 15% (Low), FPR: 20% (Low)*

The high accuracy and recall with the low FPR indicate good performance in detecting the stairs. However, most of CANUPO's predicted points were false.

- Arches Class
  - *Accuracy: 74% (Medium), Recall: 75% (Medium), Precision: 6% (Low), FPR: 26% (Low)*

Detecting arches is moderately effective, but the 6% precision is for the high rate of confusing arches with other elements. Most FP points were detected from elements with a curvature feature, like the entrance, and pointed arch windows.

- Waterspouts Class
  - *Accuracy: 91% (High), Recall: 98% (High), Precision: 3% (Low), FPR: 9% (Low)*

The very high accuracy and recall highlight CANUPO's success in identifying waterspouts. However, the low precision indicated a high number of FP points.

3.2 Northwestern Facade Evaluation Metrics

While the SW facade was used for training, the segmentation results from the NW facade are more reliable for the classifier's evaluation. It tests its ability to perform semantic segmentation on unseen data. This helps in identifying whether CANUPO is effective to use among other mosques.

- Masonry Walls Class
  - *Accuracy: 71% (Medium), Recall: 77% (High), Precision: 86% (High), FPR: 55% (Medium).*

An average performance was obtained. The high recall and precision mean it performed moderately well in detecting the correct points. However, non-targeted elements like the upper windows and the entrance were falsely classified resulting in a higher FPR.

- Windows Class
  - *Accuracy: 69% (Medium), Recall: 55% (Medium), Precision: 7% (Low), FPR: 30% (Low).*

The classifier showed moderate performance, however, it failed to detect most of the windows' geometry, especially the upper ones. These percentages illustrate failure in detecting windows from unseen data.

- Entrances Class
  - *Accuracy: 67% (Medium), Recall: 77% (High), Precision: 23% (Low), FPR: 35% (Low).*

Medium accuracy relates to the semi-high recall percentage where the classifier was able to detect 77% of the element. Yet, it had a low precision, this confusion might be caused by the element's geometry where it was confused with other elements with curvature features.

- Stairs Class
  - *Accuracy: 81% (High), Recall: 37% (Low), Precision: 3% (Low), FPR: 19% (Low).*

The high accuracy doesn't prove success in detecting the stairs, it is affected by the low FPR. A very low percentage of recall and precision demonstrates the classifier's failure to distinguish the stairs.

- Arches Class
  - *Accuracy: 72% (Medium), Recall: 99% (High), Precision: 2% (Low), FPR: 28% (Low).*

Arches scored the highest recall with almost complete identification, illustrating high success in detecting the element. What decreased the accuracy was confusing the arches with other elements.

- Waterspouts class
  - *Accuracy: 88% (High), Recall: 0% (Low), Precision: 0% (Low), FPR: 12% (Low)*

Despite the high accuracy, the 0% recall and precision percentage present a complete failure in entirely misclassifying the waterspout element. The reason behind the high accuracy is due to the waterspout's small number of points in comparison to the façade's large points number.

4. Conclusion and Suggestion

Results indicate valuable insights on the utilization of CANUPO for semantic segmentation of the Fatih mosque's facade elements. The study's objective was to address the literature's gap by creating a digital replica of the southwestern and northwestern facades and to semantically segment their elements. Based on this, a photogrammetric approach was utilized for data collection, and the CANUPO plugin for segmentation. The results showed a mix of high and medium accuracy, but it had inconsistent recall, precision, and false positive rate percentages. This chapter reflects on the validity of the findings and methodology, their implications, and potential effects.

The segmentation accuracy outcome showed a variation between high to medium accuracy. However, for classifiers with binary classification like CANUPO, high accuracy doesn't certainly present successful performance. The unexpected offsets between the evaluation metrics like the case of waterspouts from the NW facade with 88% accuracy and 0% recall, might be due to the targeted element's small points number in comparison to the nontargeted classes. However, the same class of waterspouts from the trained data had 91% accuracy proves the classifier's inconsistency and struggle to learn heritage element's features. Since this plugin was originally designed to segment vegetation and terrain, it showed a higher success with percentages near to 98% within that field (Štroner et al., 2021). However, in this study, it wasn't possible to obtain high accuracy across all elements.

The recall metric showed varying results across the elements. These random percentages partially contradict the findings of (Moyano et al., 2021), which stated that CANUPO segments bigger elements better than smaller elements. While elements like columns and arches are proportionally big with high recall, the classifier was also able to detect smaller elements of waterspouts from the SW facade with 98% recall. Yet, the classifier completely failed at segmenting the same element from unseen data, which reduces its validity for studies based on comprehensive segmentation.

In most results, the precision percentages were very low, suggesting that the classifier's predictions are usually incorrect. This might be due to the classifier not being subjected to enough data for training. This raises concerns about CANUPO's effectiveness in classifying more complex buildings with richer ornaments. On the other hand, FPR showed a low percentage for most of the elements, meaning it performed better in not misclassifying non-targeted points.

A key step to exploring CANUPO's performance was the scale ramp values set in the training phase. In this study, altering the maximum and step values is what mostly affected the segmentation results on the SW facade. Contrary to what was expected, not all values caused a noticeable outcome, especially the minimum value which caused little to no differences in classification. One possibility is that the minimum scale might be more influential for the segmentation of ornaments and smaller elements. However, the current study doesn't allow for a definitive conclusion because it didn't experiment with the segmentation of small elements. A pattern emerged in the relation between the scale ramp and the evaluation metrics percentages, where bigger elements like the main load bearing walls and columns with a larger scale range scored high recall results, meaning that CANUPO recognizes TP better when analyzing points on larger distances.

Another important aspect is the time the data was captured, where the presence of shadows affects the segmentation results and confuses the classifier into thinking that the shaded areas have different materials. Upon a trail done on the SW facade captured at 2 p.m. with the sun hitting the surface, most segmentation trails with the sun showed complete failure. Which was avoided in the other site visits. Taking that into consideration, shadow visibility wasn't an issue in this study's process.

In conclusion, this study on the utilization of CANUPO to semantically segment the Fatih Mosque's facade elements provided vital insights into its utilization within the heritage documentation and conservation field. This research aimed to segment the mosque's facade elements and provide a reliable, sharable digital model. The core problem addressed is the lack of literature and solutions for the Fatih mosque's urgent need for long-term documentation and conservation solutions. Through the implementation of point cloud semantic segmentation, this paper introduced valuable perspectives on understanding CANUPO's classifier functionality for segmenting heritage building elements.

The study's segmentation results demonstrated that the utilization of a cost-effective photogrammetric approach with the use of CANUPO served considerable potential in the extraction of digital building elements from historical buildings. Despite the challenges, this study highlighted key aspects that affect the segmentation results such as the scale ramp values and their relationship with the element's size, the capturing time, and the model's quality which all play crucial roles in the obtained results. Generally, the classifier showed inconsistent and moderate performance, calling for further developments and experiments on heritage data. Even though most segmentation results didn't achieve high accuracy, the utilized methods and workflow show potential for the use of CANUPO for semantic segmentation and heritage preservation. Concluding that with additional refinement and developments, the study's approach can be reliable for heritage digital documentation and analysis.

Future work should focus on the segmentation of smaller elements at a time, such as the segmentation of the window and the window's frame. Another focus can be the training and testing of one element repeated on multiple buildings with the same architectural style, to better understand the classifier functionality on unseen data. Moreover, elements with high accuracy can be employed within BIM to extract parametric objects. To conclude, this study presented a notable framework for the digitalization and semantic segmentation of heritage buildings' elements using CANUPO, offering a technological approach for the documentation and preservation of heritage assets in Türkiye.

Acknowledgments and Information Note

Author Contribution and Conflict of Interest Declaration Information

1st Author %65, 2nd Author %35 contributed. There is no conflict of interest.

References

Agirbas, A., Yildiz, G., & Sahin, M. (2022). Interrelation between grid systems and star polygons of muqarnas ground projection plans. *Heritage Science*, 10(1), 12. Access Address (10.09.2024): https://heritagesciencejournal.springeropen.com/articles/10.1186/s40 494-022-00647-z

Agisoft. (2019). *Agisoft Metashape*. Access Address (28.06.2024): https://www.agisoft.com/metashape/

Akyuz, T., Akyuz, S., & Gulec, A. (2015). Elemental and spectroscopic characterization of plasters from Fatih Mosque-Istanbul (Turkey) by combined micro-Raman, FTIR and EDXRF techniques. *Spectrochimica Acta Part A: Molecular and Biomolecular Spectroscopy*, *149*, 744-750. Access Address (10.09.2024): https://www.sciencedirect.com/science/article/pii/S1386142515006034

Baik, A. (2017). From point cloud to jeddah heritage BIM nasif historical house–case study. *Digital Applications İn Archaeology And Cultural Heritage*, *4*. Access Address (22.10.2024): https://www.sciencedirect.com/science/article/pii/S2212054817300073

Bal, İ. E., Gülay, F. G., Vatan, M., & Smyrou, E. (2015). Historical earthquake damages to domed structures in Istanbul. *Advances in Civil and Industrial Engineering*, 649-673. doi:10.4018/978-1-4666-8286-3.ch022. Access Address (02.11.2024): https://www.researchgate.net/publication/286932740_Historical_Earthquake_Damages_to_Domed_Structures_in_Istanbul

Barrile, V., & Fotia, A. (2022). A proposal of a 3D segmentation tool for HBIM management. *Applied Geomatics, 14*(Suppl 1), 197–209.

Berilgen, M. M. (2007). Evaluation of local site effects on earthquake damages of Fatih Mosque. *Engineering Geology, 91*(2–4), 240–253.

Beyen, K. (2008). Structural identification for post-earthquake safety analysis of the fatİH mosque after the 17 August 1999 Kocaeli earthquake. *Engineering Structures*, *30*(8), 2165-2184. Access Address (22.10.2024): https://www.sciencedirect.com /science/article/ pii/S014102960700315X

Bianchini, C. (2020). A methodological approach for the study of domes. *Nexus Network Journal*, *22*(4), 983-1013. Access Address (22.10.2024): https://www.researchgate.net/publication/ 346056413_A_Methodological_Approach_for_the_Study_of_Domes

Brodu, N., & Lague, D. (2012). 3D terrestrial LiDAR data classification of complex natural scenes using a multi-scale dimensionality criterion: Applications in geomorphology. *ISPRS Journal of Photogrammetry and Remote Sensing*, *68*, 121-134. Access Address (05.11.2024): https://www.scien cedirect.com/scienc e/article/ pii/S0924271 612000330

Champion, E., & Rahaman, H. (2019). 3D digital heritage models as sustainable scholarly resources. *Sustainability*, *11*(8), 2425. Access Address (05.09.2024): https://www.mdpi.com/2071-1050/11/8/2425

Ceylan, O. & Keleş Ocakcan, T., (2013). "Fatih Camii 2007-2012 Restorasyonu Uygulamaları." Restorasyon Yıllığı Dergisi, 7 (2013): 43-63.

Clini, P., Mariotti, C., Angeloni, R., & Muñoz Cádiz, J. (2024). Architectural heritage digital representations for conservation strategies. *The International Archives of the Photogrammetry, Remote Sensing and Spatial Information Sciences*, *XLVIII-2/W4-2024*, 111-118. doi:10.5194/isprs-archives-xlviii-2-w4-2024-111-2024. Access Address (03.04.2024): https://isprs-archives.copernicus.org/articles/XLVIII-2-W4-2024/111/2024/

Costantino, D., Pepe, M., & Restuccia, A. (2021). Scan-to-HBIM for conservation and preservation of cultural heritage building: The case study of San Nicola in Montedoro church (Italy). *Applied Geomatics*, *15*(3), 607-621. Access Address (03.04.2024): https://link.springer.com/article/10.1007/s12518-021-00359-2

Croce, V., Caroti, G., De Luca, L., Jacquot, K., Piemonte, A., & Véron, P. (2021). From the semantic point cloud to heritage-building information modeling: A semiautomatic approach exploiting machine learning. *Remote Sensing*, *13*(3), 461. Access Address (04.04.2024): https://www.mdpi.com/2072-4292/13/3/461

Ergin, A. İ. D. (2023). Digital Approach in Conservation of Heritage: 3D Virtual Reconstruction Applications in Ancient Cities. *Journal of Architectural Sciences and Applications*, 8(2), 969-987.

Eyice, S. (1995). Fatih Camii ve Külliyesi. TDV İslam Ansiklopedisi. TDV Islamic Research Center. Access Address (26.02.2025): https://islamansiklopedisi.org.tr/fatih-camii-ve-kulliyesi

Galantucci, R. A., & Fatiguso, F. (2019). Advanced damage detection techniques in historical buildings using digital photogrammetry and 3D surface analysis. *Advanced Engineering Research*, 18(3), 101-115. Access Address (10.09.2024): https://www.sciencedirect.com / science/article/abs/pii/S1296207418302528

Grilli, E., & Remondino, F. (2019). Classification of 3D digital heritage. *Remote Sensing, 11*(7), 847.

Karakus, F. (2020). Analysis of the Methods Used in Documentation of Historical Structures with Examples. *The Eurasia Proceedings of Science Technology Engineering and Mathematics*, 11, 69–76. Access Address (25.02.2025): https://dergipark.org.tr/en/down load/article-file/1434548

Kan, T., Buyuksalih, G., Ozkan, G. E., & Baskaraca, P. (2019). Rapid 3d Digitalization Of The Cultural Heritage: A Case Study On Istanbul Suleymaniye Social Complex (Kulliye). *The International Archives of the Photogrammetry, Remote Sensing and Spatial Information Sciences, XLII-2/W11*, 645–652.

Korumaz, G. A., & Dülgerler, O. N. (2011). Kültürel mirasın belgelenmesinde dijital yaklaşımlar. *S.Ü. Mühendislik-Mimarlık Fakültesi Dergisi, 26*(3), 67-83. Access Address (25.02.2025): https://dergipark.org.tr/tr/download/article-file/215784

Kuban, D. (2000). *Tarihi çevre koruma ve onarımın mimarlık boyutu: Kuram ve uygulama.* İstanbul: Yapı Endüstri Merkezi.

Kunter, H. B., & Ülgen, A. S. (1939). *Fatih camii ve Bizans sarnıcı*. Cumhuriyet Matbaası.

Macher, H., Landes, T., & Grussenmeyer, P. (2017). From point clouds to building information models: 3D semi-automatic reconstruction of indoors of existing buildings. *Applied Sciences, 7*(10), 1030.

Maiwald, F., Bruschke, J., Lehmann, C., & Niebling, F. (2019). A 4D information system for the exploration of multitemporal images and maps using photogrammetry, web technologies, and VR/AR. *Virtual Archaeology Review, 10*(21), 1–13.

Martinelli, L., Calcerano, F., Adinolfi, F., Chianetta, D., & Gigliarelli, E. (2023). Open HBIM-IoT monitoring platform for the management of historical sites and museums: An application to the Bourbon Royal Site of Carditello. *International Journal of Architectural Heritage, 1–18.*

Moyano, J., León, J., Nieto-Julián, J. E., & Bruno, S. (2021). Semantic interpretation of architectural and archaeological geometries: Point cloud segmentation for HBIM parameterisation. *Automation in Construction, 130*, 103856.

Nespeca, R., Mariotti, C., Petetta, L., & Mandriota, A. (2024). Point cloud segmentation in heritage preservation: Advanced digital process for historical houses. *The International Archives of the Photogrammetry, Remote Sensing and Spatial Information Sciences, XLVIII-2/W4-2024*, 325–332. doi:10.5194/isprs-archives-xlviii-2-w4-2024-325-2024.

Nurunnabi, A., Belton, D., & West, G. (2012). Robust segmentation for large volumes of laser scanning three-dimensional point cloud data. *IEEE Transactions on Geoscience and Remote Sensing*, 50(9), 3347–3355. doi: 10.1109/TGRS.2012.2181912, Access Address (18.09.2024): https://ieeexplore.ieee.org/abstract/document/6411672

Penjor, T., Banihashemi, S., Hajirasouli, A., & Golzad, H. (2024). Heritage Building Information Modeling (HBIM) for heritage conservation: Framework of challenges, gaps, and existing limitations of HBIM. *Digital Applications in Archaeology and Cultural Heritage, 35*, e00366.

Pierdicca, R., Paolanti, M., Matrone, F., Martini, M., Morbidoni, C., Malinverni, E. S., Frontoni, E., & Lingua, A. M. (2020). Point cloud semantic segmentation using a deep learning framework for cultural heritage. *Remote Sensing*, 12(6), 1005. doi: 10.3390/rs12061005. Access Address (12.12.2024): https://www.mdpi.com/2072-4292/12/6/1005.

Pocobelli, D. P., Boehm, J., Bryan, P., Still, J., & Grau-Bové, J. (2018). BIM for heritage science: A review. *Heritage Science, 6*(1).

Psomadaki, O. I., Dimoulas, C. A., Kalliris, G. M., & Paschalidis, G. (2019). Digital storytelling and audience engagement in cultural heritage management: A collaborative model based on the Digital City of Thessaloniki. *Journal of Cultural Heritage, 36*, 12–22.

Qi, C. R., Su, H., Mo, K., & Guibas, L. J. (2017). PointNet: Deep learning on point sets for 3D classification and segmentation. In *Proceedings of the 30th IEEE/CVF Conference on Computer Vision and Pattern Recognition (CVPR)*, 1(1), 652-660. doi: 10.1109/CVPR.2017.69. Access Address (12.12.2019): https://openaccess.thecvf.com/content_cvpr_2017 /html/Qi_PointNet_Deep_Learning_CVPR_2017_paper.html.

Qi, C. R., Yi, L., Su, H., & Guibas, L. J. (2017). PointNet++: Deep hierarchical feature learning on point sets in a metric space. In *Proceedings of the 30th Neural Information Processing Systems (NeurIPS)*, 30, 5096-5104. Access Address (12.12.2019): https://proceedings.neurips.cc/paper_files/paper/2017/file/d8bf84be3800d12f74d8b05e9 b89836f-Paper.pdf.

Rabbani, T., van den Heuvel, F. A., & Vosselman, G. (2006). Segmentation of point clouds using smoothness constraint. *ISPRS Journal of Photogrammetry and Remote Sensing*, Volume(Issue), pages. doi: d2daca8e0e381d2124455057bf3f3e94e0323e62, Access Address (20.07.2024): https://citeseerx.ist.psu.edu/document?repid=rep1&type= pdf&doi= d2daca8e0e381d2124455057bf3f3e94e0323e62

Rocha, G., Mateus, L., Fernández, J., & Ferreira, V. (2020). A scan-to-BIM methodology applied to heritage buildings. *Heritage*, *3*(1), 47-67.

Shabani, A., Skamantzari, M., Tapinaki, S., Georgopoulos, A., Plevris, V., & Kioumarsi, M. (2022). 3D simulation models for developing digital twins of heritage structures: Challenges and strategies. *Procedia Structural Integrity, 37*, 314–320.

Solla, M., Gonçalves, L. M., Gonçalves, G., Francisco, C., Puente, I., Providência, P., & Rodrigues, H. (2020). A building information modeling approach to integrate geomatic data for the documentation and preservation of cultural heritage. *Remote Sensing, 12*(24), 4028.

Stober, D., Žarnić, R., Penava, D., Turkalj Podmanicki, M., & Virgej-Đurašević, R. (2018). Application of HBIM as a research tool for historical building assessment. *Civil Engineering Journal, 4*(7), 1565.

Stouffs, R., & Tunçer, B. (2015). Typological descriptions as generative guides for historical architecture. *Nexus Network Journal, 17*(3), 785–805. https://doi.org/10.1007/s00004-015-0260-x.

Štroner, M., Urban, R., Lidmila, M., Kolář, V., & Křemen, T. (2021). Vegetation filtering of a steep rugged terrain: The performance of standard algorithms and a newly proposed workflow on an example of a railway ledge. *Remote Sensing, 13*(15), 3050.

Themistocleous, K., Evagorou, E., Mettas, C., & Hadjimitsis, D. G. (2022). The use of digital twin models to document cultural heritage monuments. *Earth Resources and Environmental Remote Sensing/GIS Applications XIII, 13*.

Vatan, M. (2018). Lessons learned from earthquake damage to masonry domed monuments in Istanbul. Z. Ahunbay, D. Mazlum, & Z. Eres (Ed.), *Conservation of cultural heritage in Turkey* (67–84). ICOMOS Turkey.

Xie, Y., Tian, J., & Zhu, X. X. (2020). Linking points with labels in 3D: A review of point cloud semantic segmentation. *IEEE Geoscience and Remote Sensing Magazine, 8*(4), 38–59.

Yang, S., Hou, M., & Li, S. (2023). Three-dimensional point cloud semantic segmentation for cultural heritage: A comprehensive review. *Remote Sensing, 15*(3), 548.

Yastıklı, N., & Alkıs, Z. (2003). Documentation of cultural heritage by using digital close range photogrammetry. In *Proceedings of XIX th International Symposium CIPA, New Perspective to Save Cultural Heritage*.